RESEARCH PAPER

Inhibition of transmembrane member 16A calcium-activated chloride channels by natural flavonoids contributes to flavonoid anticancer effects

Correspondence Professor Wei Zhang, Department of Pharmacology, Institution of Chinese Integrative Medicine, Hebei Medical University, No.361 East Zhongshan Road, Shijiazhuang, Hebei 050017, China, and Dr Xuan Zhang, Department of Pharmacology, Hebei University of Chinese Medicine, No.326 South Xinshi Road, Shijiazhuang, Hebei 050091, China. E-mail: weizhang@hebmu.edu.cn; xuan_zhangt@hotmail.com

Xuan Zhang[1,2,*] (iD), Honglin Li[3,*], Huiran Zhang[3], Yani Liu[4], Lifang Huo[1], Zhanfeng Jia[4], Yucong Xue[2], Xiaorun Sun[2] and Wei Zhang[1]

[1]Department of Pharmacology, Institution of Chinese Integrative Medicine, Hebei Medical University, Shijiazhuang, China, [2]Department of Pharmacology, Hebei University of Chinese Medicine, Shijiazhuang, China, [3]Department of Respiratory, The Second Hospital of Hebei Medical University, Shijiazhuang, China, and [4]Department of Pharmacology, Hebei Medical University, Shijiazhuang, China

*Both authors contributed equally to this work.

BACKGROUND AND PURPOSE

Natural flavonoids are ubiquitous in dietary plants and vegetables and have been proposed to have antiviral, antioxidant, cardiovascular protective and anticancer effects. Transmembrane member 16A (TMEM16A)-encoded Ca^{2+}-activated Cl^- channels play a variety of physiological roles in many organs and tissues. Overexpression of TMEM16A is also believed to be associated with cancer progression. Therefore, inhibition of TMEM16A current may be a potential target for cancer therapy. In this study, we screened a broad spectrum of flavonoids for their inhibitory activities on TMEM16A currents.

EXPERIMENTAL APPROACH

A whole-cell patch technique was used to record the currents. The BrdU assay and transwell technique were used to investigate cell proliferation and migration.

KEY RESULTS

At a concentration of 100 μM, 10 of 20 compounds caused significant ($>50\%$) inhibition of TMEM16A currents. The four most potent compounds - luteolin, galangin, quercetin and fisetin – had IC_{50} values ranging from 4.5 to 15 μM). To examine the physiological relevance of these findings, we also studied the effects of these flavonoids on endogenous TMEM16A currents in addition to cell proliferation and migration in LA795 cancer cells. Among the flavonoids tested, we detected a highly significant correlation between TMEM16A current inhibition and cell proliferation or reduction of migration.

CONCLUSIONS AND IMPLICATIONS

This study demonstrates that flavonoids inhibit TMEM16A currents and suggests that flavonoids could have anticancer effects *via* this mechanism.

Abbreviation

CaCC, Ca^{2+}-activated Cl^- channel

Introduction

Based on their chemical structures, flavonoids, a class of natural polyphenolics, are classified into flavonols, flavones, flavanones, isoflavones, catechins, anthocyanidins and chalcones. They are ubiquitous in dietary plants and vegetables; quercetin, myricetin, kaempferol and fisetin are the most common flavonoids and are very prevalent in onions, apples, strawberry, molokheka and grape (Arai *et al.,* 2000). Flavonoids have been proposed to have multiple health benefits such as antiviral, antioxidant, anti-inflammatory and anticancer and cardiovascular protection (Croft, 1998). Epidemiological studies suggest that dietary intake of flavonoids is inversely associated with the risk of lung, prostate, stomach and breast cancer (Knekt *et al.,* 1997; Garcia-Closas *et al.,* 1998; Hirvonen *et al.,* 2001; Neuhouser, 2004; Wright *et al.,* 2004).

Transmembrane protein 16A (TMEM16A), also known as anoctamin-1 (ANO1 or DOG1), was identified as one of several endogenous **Ca^{2+}-activated Cl^- channels (CaCCs)** and shown to have a variety of physiological roles in many organs and tissues (Caputo *et al.,* 2008; Schroeder *et al.,* 2008; Yang *et al.,* 2008). Accumulating evidence shows that TMEM16A is frequently up-regulated in many types of human tumours, including squamous cell head and neck carcinomas, gastrointestinal stromal tumours, gastric, breast, bladder and esophageal cancers (Akervall *et al.,* 1995; West *et al.,* 2004; Carneiro *et al.,* 2008; Britschgi *et al.,* 2013; Liu *et al.,* 2015). Overexpression of TMEM16A correlated with tumour proliferation, migration and decreasing patient survival, while knock-down TMEM16A by siRNA or application of CaCC blockers significantly inhibited tumour growth and progression (Duvvuri *et al.,* 2012; Mazzone *et al.,* 2012; Ruppersburg and Hartzell, 2014). Therefore, TMEM16A may be a putative diagnostic and prognostic biomarker for certain human cancers. In addition, TMEM16A may be a potential pharmacological target for cancer therapy.

Low MW compounds have been developed as TMEM16A inhibitors. T16A$_{inh}$-A01, an aminophenylthiazole compound, was found to be a specific TMEM16A inhibitor with an IC$_{50}$ of 1.1 μM (Namkung *et al.,* 2010a), which inhibited the proliferation of a TMEM16A-expressing human pancreatic cancer cell line (Mazzone *et al.,* 2012). Another compound, CaCC$_{inh}$-A01 (De La Fuente *et al.,* 2008), and a natural product, **tannic acid** (Namkung *et al.,* 2010b), have also been reported to inhibit TMEM16A-encoded CaCCs.

In the present study, we identified several flavonoids that inhibited TMEM16A currents and demonstrated structure–activity relationships. Moreover, our results also provide evidence that TMEM16A inhibition by flavonoids may be responsible for flavonoid-associated anticancer effects.

Methods

cDNA and cell lines

Plasmids encoding mouse TMEM16A (GenBank accession number: NM_178642.5) was kindly provided by Prof Uhtaek Oh (Seoul National University, Korea) and was subcloned into expression vector pEGFPN1.

CHO cells stably transfected with TMEM16A were kindly provided by Professor Hailin Zhang (Department of Pharmacology, Hebei Medical University, Shijiazhuang, China). LA795 cells were purchased from the Cell Bank of the Chinese Academy of Sciences (Shanghai, China). The normal lung 2BS cell line was kindly provided by Prof Kewei Wang (Department of Pharmacology, Qingdao University School of Pharmacy, Qingdao, China). The 2BS cell line was originally obtained from the National Institute of Biological Products (Beijing, China).

Cell culture

CHO cells, LA795 cells, HEK293 cells and normal lung 2BS cells were cultured in F-12K (Solarbio, China) (1% nonessential amino acids, 600 μg·mL⁻¹ G418), RPMI 1640 (Solarbio, China) or DMEM medium (Solarbio, China) supplemented with 10% fetal bovine serum (Gibco, USA) and antibiotics (100 IU·mL⁻¹ penicillin G and 100 mg·mL⁻¹ streptomycin; Solarbio, China) in a humidified incubator at 37°C and 5% CO₂. Cells were seeded on glass coverslips in a 24-multiwell plate. Recordings were made 12 h after cells were seeded, and cells were used within 48 h.

Electrophysiology

Whole-cell patch recordings were performed on CHO or LA795 cells. Recordings were made at room temperature (23–25°C). Pipettes were pulled from borosilicate glass capillaries with resistances of 2–3 MΩ when filled with internal solution. Currents were recorded using an Axon patch 700B amplifier and pClamp 10.0 software (Axon Instruments, Foster City, CA, USA). The access resistance in our experiments was approximately 7–12 MΩ, and 60–80% series resistance compensation was achieved. Current records were acquired at 5 kHz and filtered at 2 kHz. The external solution used to record TMEM16A currents contained the following (in mM): 160 NaCl, 2.5 KCl, 2 CaCl₂, 1 MgCl₂, 10 HEPES and 8 glucose, pH 7.4. The internal solution contained the following (in mM): 130 CsCl, 10 EGTA; 1 MgCl₂, 10 HEPES, 2 ATP, pH 7.3 and different concentrations of CaCl₂ to obtain the desired free Ca²⁺ concentration (1 mM for 12 nM and 7 mM for 384 nM). Free Ca²⁺ concentration was calculated using the Webmaxc software (Stanford; http://www.stanford.edu/~cpatton/webmaxc/webmaxcS.htm).

A voltage ramp from −100 to +100 mV over 4 s was used to record the whole-cell TMEM16A currents (Figure 1C, top). Drug effects were quantified by measuring the drug-induced changes in current amplitude at +100 mV. Current–voltage (I–V) relationships were determined using step pulses between −100 and +100 mV in increments of 10 mV from a holding potential of 0 mV followed by a −100 mV step (Figure 3B, top). The currents were recorded until the effects had stabilized. This normally takes 5–15 min (Figures 1C and 4D). Current amplitudes were measured at +100 mV.

Western blot analysis

Control and stably transfected CHO, LA795 and HEK293 cells were harvested in lysis buffer (20 mM Tris-base, 137 mM NaCl, 10% glycerol, 1% Triton-X-100, 2 mM EDTA and 1 μL·mL⁻¹ protease inhibitor), and lysates were centrifuged at 17200× *g* for 30 min; pellets were then discarded. Protein samples were heated to 70°C for 10 min in SDS-PAGE loading
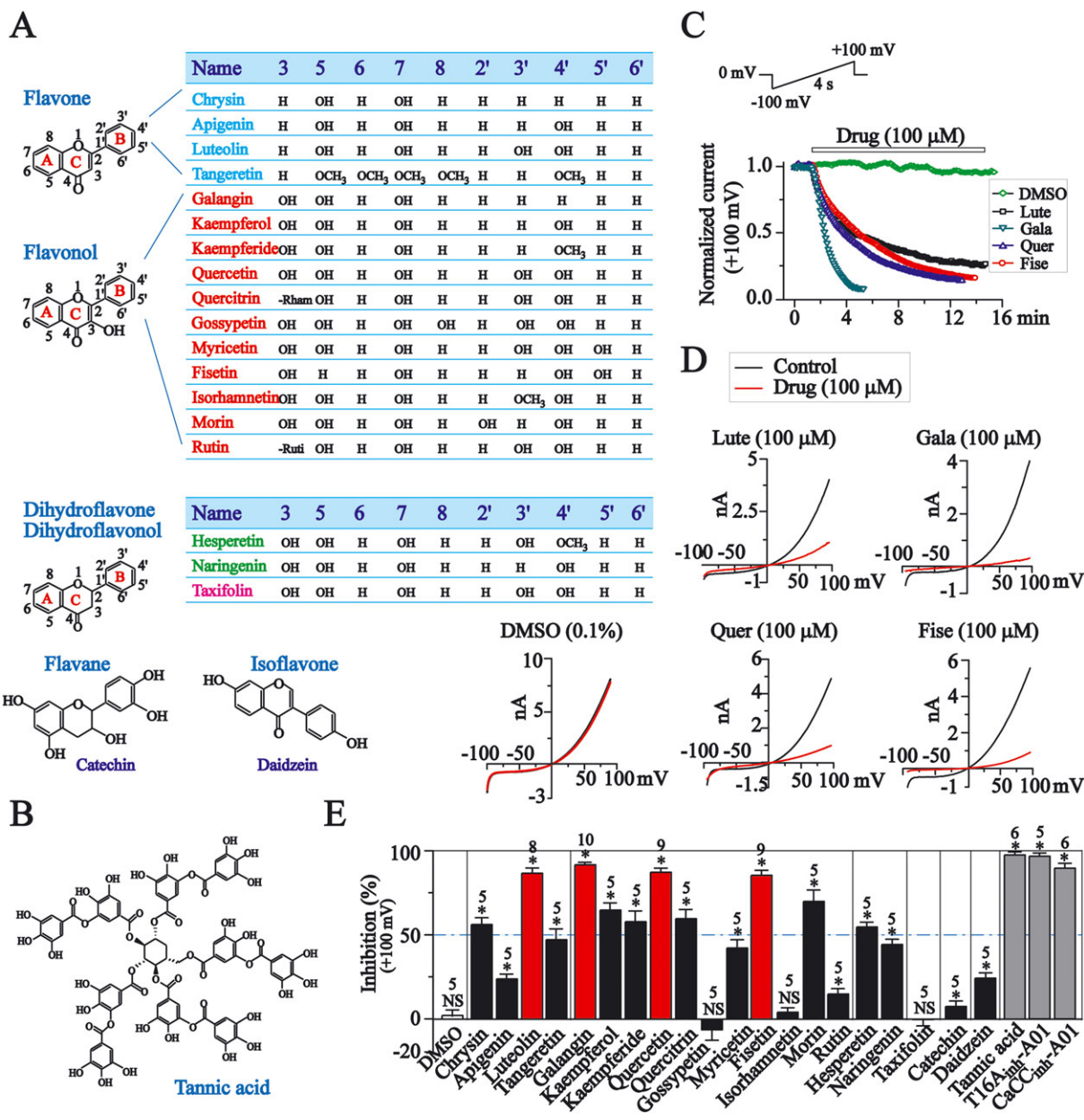
Figure 1

The effects of flavonoid compounds on recombinant TMEM16A currents in CHO cells. (A) Chemical structures of flavonoids. (B) Chemical structures of tannic acid. (C) The time course for the effects of **luteolin** (Lute), **galangin** (Gala), **quercetin** (Quer) and **fisetin** (Fise), all at 100 μM and DMSO (0.1%) on TMEM16A currents tested at +100 mV. The protocol was shown at the top of the figure. (D) The representative current traces recorded when the effect of drugs has stabilized. (E) The inhibition by flavonoids (100 μM), DMSO (0.1%), tannic acid, T16Ainh-A01 and CaCCinh-A01 (100 μM) of TMEM16A current tested at +100 mV. NS, not significant; *$P < 0.05$, significant effect of treatments.

buffer and separated on a 10% polyacrylamide gel. The separated proteins were transferred at 30 V to nitrocellulose membrane (Millipore, USA) overnight at 4°C. After blocking the membrane in Tris-buffered saline (TBS) containing 5% non-fat milk, the blots were incubated with primary antibodies at room temperature for 4–6 h. Antibodies were used at a 1:500 dilutions and consisted of polyclonal anti-TMEM16A (rabbit; Santa Cruz Biotechnology, USA), polyclonal anti-TMEM16A (rabbit; Santa Cruz Biotechnology, USA) and monoclonal anti-β-tubulin III

(mouse; Sigma, USA). After incubation with primary antibodies, membranes were rinsed with Tris-buffered saline Tween 20 (TBST; 150 mM NaCl, 20 mM Tris-base, 0.05% Tween-20) three times for 10 min and then incubated with secondary antibodies at room temperature for 1–2 h. Membranes were washed twice with TBST for 10 min per wash and once with TBS for 10 min. Protein bands were visualized using an ECL system (Amersham Biosciences, Piscataway, NJ, USA) and quantified by densitometry using a Bio-profile Bio, ID image analyser.
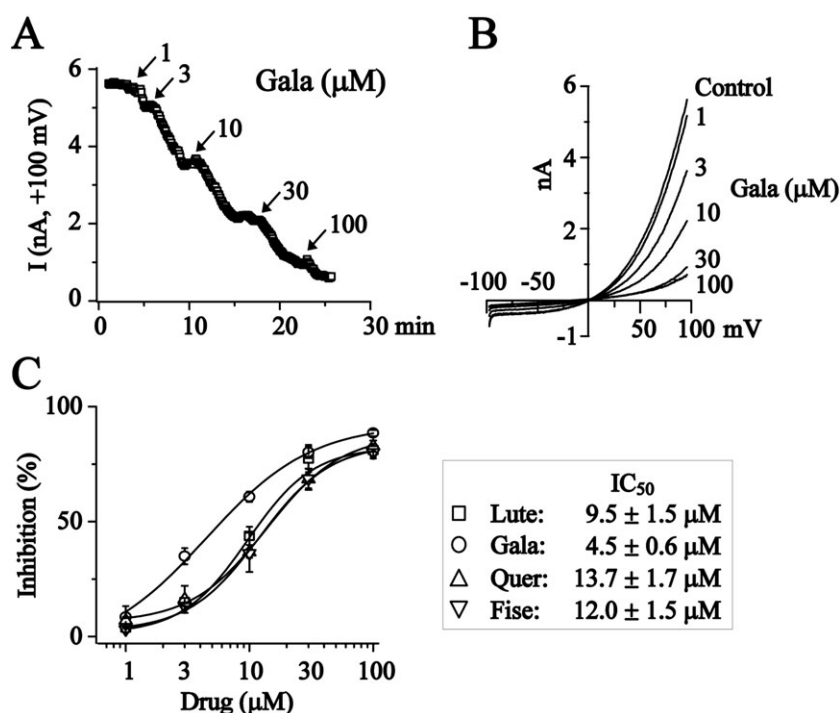
Figure 2

The concentration–response relationships for **luteolin** (Lute), **galangin** (Gala), **quercetin** (Quer) and **fisetin** (Fise) on recombinant TMEM16A currents in CHO cells. (A) The time course for the effects of **galangin** (1–100 μM) on TMEM16A currents tested at +100 mV. (B) The representative current traces recorded when the effect of different concentrations of **galangin** had stabilized. (C) Concentration–response relationships for **luteolin**, **galangin**, **quercetin** and **fisetin** on TMEM16A currents recorded at +100 mV. Data were fitted with logistic function. L**uteolin**: $n = 5, 5, 5, 5$ and 8; **galangin**: $n = 5, 5, 9, 5$ and 7; **quercetin**: $n = 5, 5, 5, 7$ and 9; **fisetin**: $n = 5, 5, 5, 6$ and 9 (1, 3, 10, 30 and 100 μM).

Immunofluorescence

LA795 cells were seeded on glass coverslips in a 24-multiwell plate. Cells were fixed with 10% formalin when 60–70 % confluence was reached, permeabilized with 0.2% Triton-X-100 and labelled with anti-TMEM16A (Santa Cruz Biotechnology, USA) and antigoat-conjugated cy3, anti-α-tubulin (Affinity Biotechnology, USA) and anti-rabbit-conjugated FITC. Hoechst (1:4000) staining was used to identify nuclei. Confocal images were taken with Olympus Fluoview Fvl000 Microsystems. TMEM16A fluorescence intensity was analysed by the ImageJ system (Li *et al.*, 2016).

BrdU cell proliferation assay

Flavonoids and tannic acid were tested for their effects on the proliferation of LA795, HEK293 and normal lung 2BS cells. Cells were plated on 96-well microplates. Twelve hours after seeding, cells were treated with different concentrations of flavonoids or tannic acid (10, 30 and 100 μM). After 24 h incubation, the cells were incubated with BrdU (100 μM) for 4 h. The incorporation of BrdU into DNA was measured according to the supplier's instructions of the BrdU Cell Proliferation Assay Kit (Millipore, MA, USA). Optical density readings were made at 450 nm. Cells not exposed to flavonoids or tannic acid served as the negative control (NC). All measurements were repeated three times, and proliferation values were calculated relative to the NC whose viability was set to 100%.

Transwell assay

LA795 cells were plated in 8.0 μm pore size transwell 24-insert plate chambers (Corning, Acton, MA, USA) coated with BioCoatMatrigel (BD Biosciences, Bedford, MA, USA). After pre-starving for 24 h by culturing in serum free medium, 3×10^4 LA795 cells per well were plated in the upper chambers with serum free medium and incubated for 24 h. The lower chambers were filled with medium containing 10% FBS. After wiping off the cells from the upper side of the upper chamber, the lower side of the upper chamber was fixed with methanol and stained with 4,6-diamidino-2-phenylindole (DAPI; Sigma).

Data and statistical analysis

The data and statistical analysis in this study comply with the recommendations for experimental design and analysis in pharmacology (Curtis *et al.*, 2015). Blinding was not used in the experiments since all measurements were not subjective but were strictly based on quantitative data. Randomization was not used in the experiments since the inhibitory effects of flavonoids on TMEM16A currents were obtained by comparing the currents before (control) and after drug application.

Currents were analysed and then curve fitted using Clampfit 10.2 (Molecular Devices, Sunnyvale, CA, USA) and Origin 7.5 (OriginLab Corp., Northampton, MA, USA) software. The concentration–response curve was
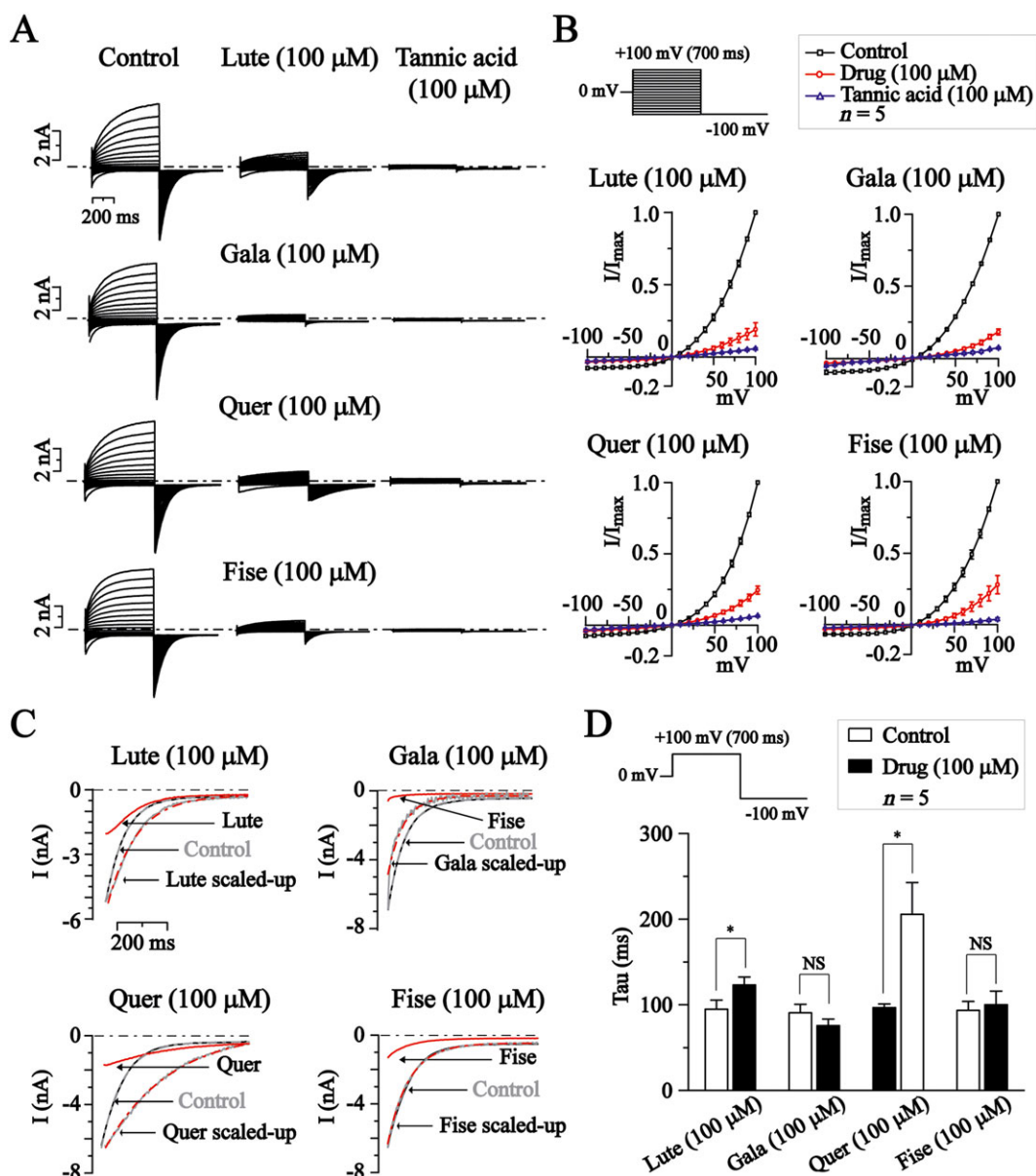
Figure 3

The effects of **luteolin** (Lute), **galangin** (Gala), **quercetin** (Quer) and **fisetin** (Fise) on I–V relationship and deactivation kinetics of TMEM16A currents in CHO cells. (A) Representative traces of TMEM16A currents recorded using the voltage protocol indicated at the top of B. Dotted lines indicated the zero current level. The effects of **luteolin**, **galangin**, **quercetin** and **fisetin** (all at 100 μM) or tannic acid (100 μM) are shown. (B) Normalized current–voltage relationships of TMEM16A currents in the absence or presence of the compounds; $n = 5$ for each experimental group. (C) The effects of **luteolin**, **galangin**, **quercetin** and **fisetin** on the deactivation kinetics of TMEM16A currents from +100 to −100 mV. The red line shows the deactivating currents in the presence of the compounds, which were scaled up to match the amplitude of the deactivating currents in the absence of the compounds. (D) Summary of effects of **luteolin**, **galangin**, **quercetin** and **fisetin** on the time constants of TMEM16A deactivating currents. *$P < 0.05$, significantly different from control, $n = 5$ for each experimental group.

fitted with logistic equation: $y = A_2 + (A_1–A_2)/[1 + (x/x_0)^p]$, in which y is the response; A_1 and A_2 are the maximum and minimum responses, respectively, x is the drug concentration, x_0 is the EC_{50} and p is the Hill coefficient. To analyse the kinetics of TMEM16A current deactivation, the tail currents deactivating from +100 to −100 mV were used to obtain the time constants. The deactivation traces were fitted to a single exponential

function: $I = A \times [1 − \exp(−t/\tau)] + I_0$, in which I is the current, I_0 is the steady-state amplitude of the current at the end of the holding potential of −100 mV, A is the difference between the peak and steady-state current amplitudes, t is time and τ is the time constant.

Data normalization was used in the test of the drug effects on the current–voltage (I–V) relationships (Figures 3B and 5B). Current amplitude was normalized by testing the current
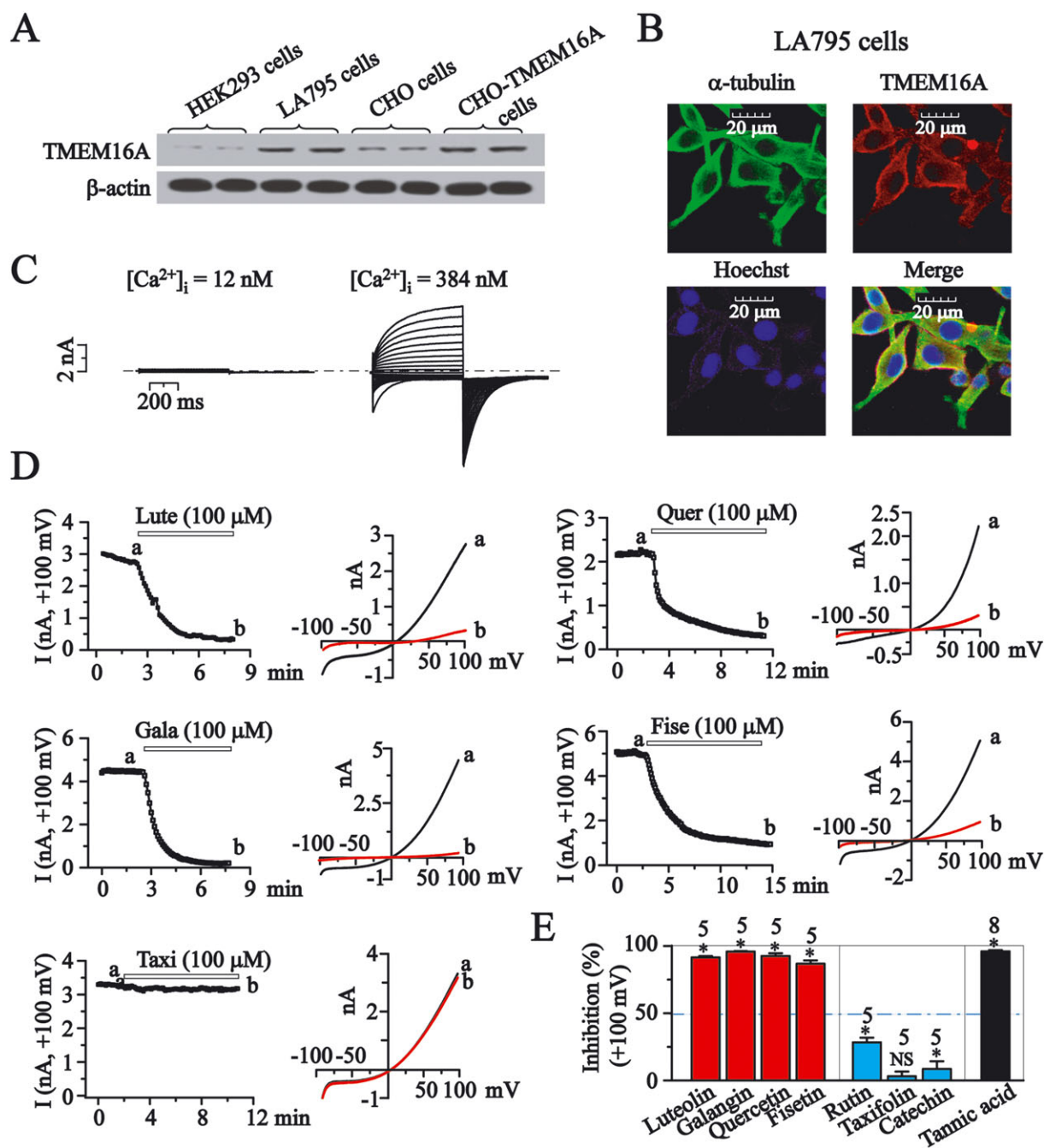
Figure 4

The effects of flavonoids on endogenous TMEM16A currents in LA795 cells. (A) Western blots of TMEM16A protein levels. (B) The expression of endogenous TMEM16A in LA795 cells. Cells were stained with anti-α-tubulin (green) and anti-TMEM16A antibodies (red). Nuclei were stained with Hoechst (blue). (C) Whole-cell currents at the indicated intracellular free Ca^{2+} concentrations in LA795 cells. (D) The time course for the effects of **luteolin** (Lute), **galangin** (Gala), **quercetin** (Quer) and **fisetin** (Fise) and taxifolin (Taxi), all at 100 μM on TMEM16A currents tested at +100 mV. The protocol was shown at the top of the Figure 1B. The representative current traces recorded when the effect of the compounds had stabilized. (E) The inhibition by flavonoids (100 μM) of TMEM16A current tested at +100 mV. NS, not significant, *$P < 0.05$, significant effect of treatments.

at +100 mV in the absence of the drugs (control) in order to reduce the unwanted sources of variation. All data are presented as mean ± SEM. Statistical analyses were performed using a two-sample paired Student's *t*-test or one-way ANOVA. The differences were considered significant at $P < 0.05$. In cases in which ANOVA was used, a *post hoc* test (Bonferroni) was used, if F achieved $P < 0.05$, and there was no significant variance inhomogeneity. The current
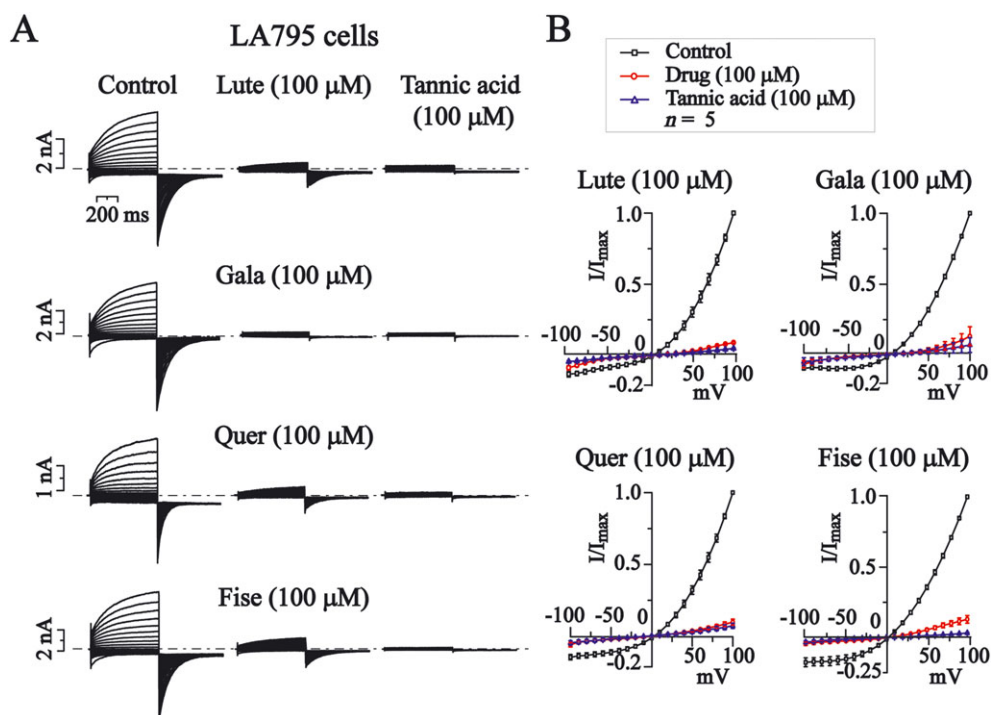
Figure 5

The effects of **luteolin** (Lute), **galangin** (Gala), **quercetin** (Quer) and **fisetin** (Fise), on I–V relationship of TMEM16A currents in LA795 cells. (A) Representative traces of TMEM16A currents recorded using the voltage protocol indicated in the top of Figure 3B. Dotted lines indicated the zero current level. The effects of **luteolin**, **galangin**, **quercetin** and **fisetin** (100 μM) or tannic acid (100 μM) are shown. (B) Normalized current–-voltage relationships of TMEM16A currents in the absence or presence of the drugs; *n* = 5 for each experimental group.

amplitudes (or τ values) before and after drug treatment were compared with a two-sample paired Student's *t*-test (Figures 1E, 3D and 4E). Drug treatment effects on cell proliferation/migration were analysed by one-way ANOVA.

Materials

Chrysin, **apigenin**, **luteolin**, tangeretin, **galangin**, kaempferol, kaempferide, **quercetin**, quercitrin, gossypetin, myricetin, **fisetin**, isorhamnetin, **morin**, rutin, hesperetin, naringenin, taxifolin, catechin and **daidzein** were purchased from J&K China Chemical Ltd. (Beijing, China). Tannic acid was purchased from Sigma-Aldrich Corp (St. Louis, MO, USA). The stock solutions were made in DMSO and were stored at −20°C. All solutions were freshly prepared from stock solutions before each experiment and kept from light exposure. The final concentration of DMSO was less than 0.1%.

Nomenclature of targets and ligands

Key protein targets and ligands in this article are hyperlinked to corresponding entries in http://www.guidetopharmacology.org, the common portal for data from the IUPHAR/BPS Guide to PHARMACOLOGY (Southan *et al.*, 2016), and are permanently archived in the Concise Guide to PHARMACOLOGY 2015/16 (Alexander *et al.*, 2015).

Results

Natural flavonoid compounds inhibit the recombinant TMEM16A currents in CHO cells

We compared 20 flavonoids for their inhibitory activities against recombinant TMEM16A currents; these compounds included flavones (chrysin, apigenin, luteolin and tangeretin), flavonols (galangin , kaempferol, kaempferide, quercetin, quercitrin, gossypetin, myricetin, fisetin, isorhamnetin, morin and rutin), dihydroflavones (hesperetin and naringenin), dihydroflavonol (taxifolin; also named dihydroquercetin), a flavane (catechin) and an isoflavone (daidzein) (Figure 1A). The inhibitory effects were compared with those of three known blockers of TMEM16A currents: (1) T16Ainh-A01 (Supporting Information Figure **S1**A, Namkung *et al.*, 2010a); (2) CaCCinh-A01 (Figure **S1**A, De La Fuente *et al.*, 2008); and (3) tannic acid (Figure 1B, Namkung *et al.*, 2010b).

A voltage ramp from −100 to +100 mV over 4 s was used to record the whole-cell recombinant TMEM16A currents in CHO cells (Figure 1C, top). The TMEM16A currents were activated with 384 nM free intracellular Ca²⁺. The effects of four flavonoids (luteolin, galangin, quercetin, fisetin) each at 100 μM, were quantified by measuring the changes of amplitude at +100 mV induced by these drugs (Figure 1C, D).

At the concentration of 100 μM, 10 of the 20 compounds significantly inhibited (>50%) TMEM16A currents by, including chrysin, luteolin, galangin, kaempferol,

kaempferide, quercetin, quercitrin, fisetin, morin and hesperetin (Figure 1E). Among these compounds, luteolin, galangin, quercetin and fisetin exhibited the highest efficacy for TMEM16A channel blockade (Figure 1E). At the same concentration (100 μM), the reference inhibitors, tannic acid, T16Ainh-A01 and CaCCinh-A01 blocked TMEM16A currents almost completely (Figure 1E).

The effects of luteolin, galangin, quercetin and fisetin on recombinant TMEM16A currents

Because of their strong inhibitory effects, four of the 20 flavonoids, luteolin, galangin, quercetin and fisetin (Figure 2A), were studied further for their inhibitory activity on recombinant TMEM16A currents in CHO cells.

A concentration-dependent relationship was established. In these experiments, TMEM16A currents activated at +100 mV in the presence of different concentrations of these compounds were tested. As demonstrated in Figure 2A, B, TMEM16A currents were inhibited by galangin in a concentration-dependent manner. The concentration–response curves were fitted with a logistic function and the IC_{50} and the E_{max} values for these compounds is shown in Figure 2C.

I–V curves for voltage-dependent activation of TMEM16A currents were established from the active currents. The currents were elicited by voltage pulses switching from a holding potential of 0 mV to voltages between −100 and +100 mV in 10 mV steps followed by a step to −100 mV as indicated at the top of Figure 3B (Figure 3A). Figure 3B shows the normalized I–V curves of TMEM16A currents + compounds (100 μM). The effects were compared with those of tannic acid (100 μM).

We then examined these drugs using the time constants (τ values) of the deactivating tail currents at −100 mV. The deactivation of the TMEM16A tail currents was significantly slowed by quercetin and luteolin, but not by galangin or fisetin (100 μM, Figure 3C). The τ values for the four compounds are shown in Figure 3D.

The effects of flavonoids on endogenous TMEM16A currents in LA795 cells

Additional evidence suggests that overexpression of TMEM16A is closely associated with cell proliferation, metastasis and apoptotic sensitivity in cancer tissues (Qu et al., 2014). In this set of experiments, we examined the expression and function of TMEM16A in LA795 cells (mouse lung adenocarcinoma cells) and tested the flavonoids for modulatory effects on endogenous TMEM16A currents.

The protein expression of TMEM16A in LA795 cells was confirmed by Western blot. We found TMEM16A mainly localized to the plasma membrane (Figure 4A, B). In addition, the activation of outward currents in LA795 cells was dependent on the intracellular Ca^{2+} concentration (Figure 4C). These results demonstrated that TMEM16A channels were functional in LA795 cells. At 100 μM, luteolin, galangin, quercetin and fisetin caused marked inhibition of TMEM16A currents, while rutin and catechin showed slight effects, and taxifolin did not affect the currents (Figure 4D, E). Tannic acid (100 μM) induced almost complete inhibition (Figure 4E).

We then examined the effects of luteolin, galangin, quercetin and fisetin on I–V curves of TMEM16A currents in these cells. Figure 5B showed the normalized I–V curves of TMEM16A currents ,with or without the compounds at 100 μM. The effects were then compared with those of tannic acid (100 μM).

The effects of flavonoids on cell proliferation and migration in LA795 cells

Next, we examined the effects of flavonoids on proliferation and migration of LA795 cells.

Luteolin, galangin, quercetin and fisetin, which had demonstrated significant inhibitory effects on TMEM16A currents, also significantly inhibited cellular proliferation in a dose-dependent manner (Figure 6A). Rutin, catechin and taxifolin, which had minimal inhibitory effects on TMEM16A currents, demonstrated limited effects on cell proliferation (Figure 6A). We also tested the effects of these flavonoids on normal lung 2BS cells and wild-type HEK293 cells. Luteolin, galangin, quercetin and fisetin demonstrated
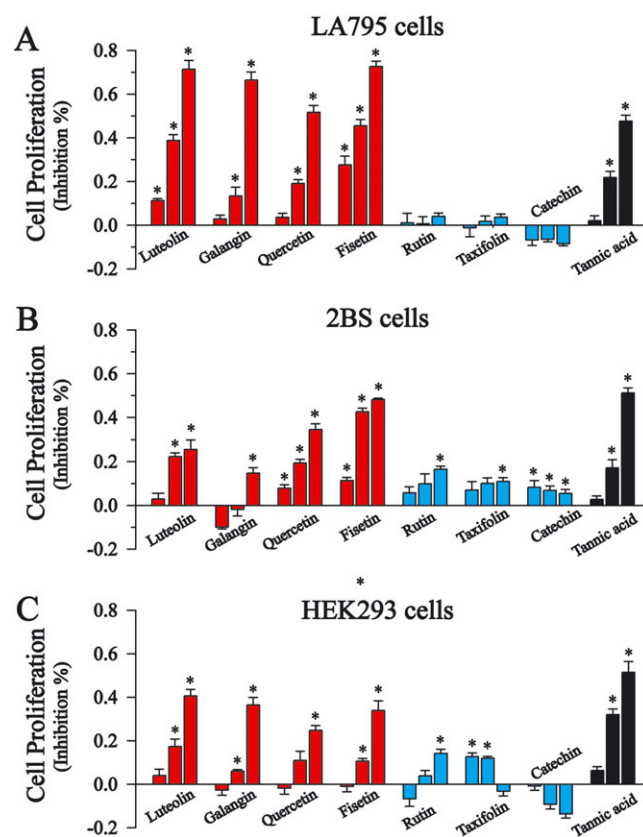

Figure 6

The effects of flavonoids on cell proliferation in LA795 cells. (A–C) LA-795, normal lung 2BS and wild-type HEK293B cells seeded in 96-well plates were treated with flavonoids (100 μM) or tannic acid (100 μM) for 24 h as indicated. The results represent the means of three independent experiments. Proliferation rate of untreated cells was set to 100%. NS, not significant, *$P < 0.05$, significant effect of treatments.

weaker inhibition of cell proliferation, compared with their effects on LA795 cells (Figure 6B, C). These results indicate that these flavonoids exhibited greater cytotoxicity towards the cancer cell line than they did on the normal cell lines.

To assess the effects of flavonoids on LA795 cell migration, the transwell migration assay was used. Luteolin, galangin, quercetin and fisetin also demonstrated inhibitory effects, while rutin, taxifolin and catechin demonstrated limited effects in this migration assay (Figure 7A, B). Taking these results together, it appears that inhibition of endogenous TMEM16A currents by flavonoids contributes to the anticancer effects of the flavonoids, demonstrated in LA795 cells.

Discussion

In the present study, we have demonstrated that several natural flavonoids inhibited the TMEM16A-encoded CaCCs and also have described some structure–activity relationships of these compounds. Furthermore, our results also demonstrate for the first time that TMEM16A inhibition by flavonoids may contribute to their anticancer effects.

Before the TMEM16A channels were cloned, conventional non-selective anion channel blockers such as **NPPB**, **DIDS**, niflumic acid (NFA) and flufenamic acid (FFA) were used as pharmacological tools in CaCC studies. However, these blockers appear to be non-selective and also affect other channels. For example, NPPB and DIDS have been reported to also inhibit volume-regulated anion channels (Helix et al., 2003; Parkerson and Sontheimer,

2004; Zhang et al., 2011). DIDS also inhibits renal CLC-K1 (Liantonio et al., 2004) and CLC-Ka (Picollo et al., 2004) Cl^- channels and potentiates capsaicin-induced TRPV1 currents (Zhang et al., 2012). NPPB, DIDS, NFA and FFA inhibit bestrophin-1 Cl^- channels (Liu et al., 2014). Recently, T16A$_{inh}$-A01 (Namkung et al., 2010a), CaCC$_{inh}$-A01 (De La Fuente et al., 2008), the natural compound tannic acid (Namkung et al., 2010b) and quercetin (Gim et al., 2015) have been reported to inhibit TMEM16A channels. T16A$_{inh}$-A01 has shown better selectivity on TMEM16A channels. The present work demonstrated the inhibitory effects of several natural flavonoids on TMEM16A channels and our data provides evidence that these compounds may be developed into new TMEM16A-specific CaCC inhibitors.

Flavonoids are the most important class of phenolic compounds. They have a common structure of two aromatic rings connected to three carbon atoms (C6′C3′C6, Figure 1A). Our data indicated several important structure –activity findings: (1) non-glycosylated derivatives such as **luteolin**, **galangin**, **quercetin** and **fisetin** displayed a greater inhibition of TMEM16A currents than the related flavonoids, quercitrin and rutin; (2) the absence of the double bond at positions C-2/C-3 deletes the TMEM16A blocking effect of the flavanone, taxifolin, in contrast to the flavonol quercetin; (3) the presence of a second hydroxyl group at the C-3′ of B ring on the structure of **quercetin** or **luteolin** increased its efficiency in comparison with kaempferol or apigenin; (4) the presence of a third hydroxyl group at the C-5′ of B ring on the structure of myricetin decreased its efficiency in comparison with **quercetin**; (5) the presence of a hydroxyl
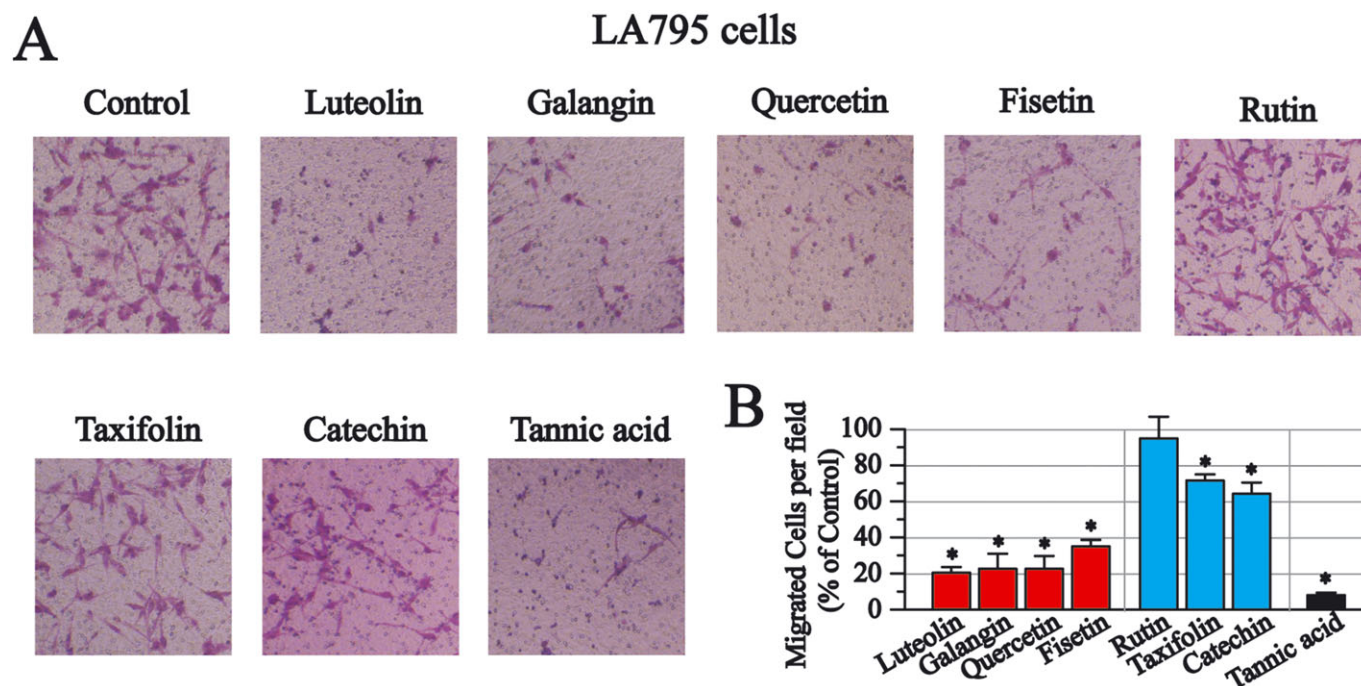

Figure 7
The effects of flavonoids on cell migration in LA795 cells. (A) Transwell migration assay. Representative images after flavonoids (30 μM) or tannic acid (30 μM) treatment for 24 h. (B) Summary results. NS, not significant, *$P < 0.05$, significant effect of treatments.

group at the C-3 of C ring on the structure of **galangin**, kaempferol or **quercetin** increased its efficiency in comparison with chrysin or apigenin; (6) the presence of a hydroxyl group at the C-5 of A ring on the structure of quercetin slightly affected its efficiency in comparison with **fisetin**; (7) substituting the hydroxyl group at the C-3′ of B ring with a methoxy group (isorhamnetin) deletes the activity of quercetin; and (8) the deactivation of the TMEM16A tail currents was significantly slowed by **quercetin** and **luteolin**, but not by **galangin** or **fisetin** (Figure 3C, D), which might be attributed by the presence of a second hydroxyl group at the C-3′ of B ring.

The anticancer activity of flavonoids has been described in many studies, and almost as many mechanisms appear to be involved. Recently, TMEM16A channels have been closely associated with development of some types of cancer. Our results indicate that **luteolin**, **galangin**, **quercetin** and **fisetin** potently inhibited cancer cell proliferation and migration (Figures 6 and 7), which significantly corresponds with the effects of these compounds on endogenous TMEM16A currents in LA795 cells (Figure 4). In contrast, rutin, taxifolin and catechin, which have little or no inhibitory effects on TMEM16A currents, showed lesser anticancer effects, as shown in Figures 4, 6 and 7. The data indicate that inhibition of TMEM16A currents by flavonoids may contribute to the anticancer activities of flavonoids . In addition, **luteolin**, **galangin**, **quercetin** and **fisetin** exhibited weaker growth inhibition in wild-type HEK293 cells, than in LA795 cells (Figure 6B). In contrast, although tannic acid has stronger inhibitory effects on TMEM16A currents, it shows weaker effects on cell proliferation in LA795 cells (Figures 4 and 6). Furthermore, tannic acid showed unexpectedly higher inhibition of proliferation in HEK293 cells (Figure 6). In summary, compared with tannic acid, flavonoids appear to have more potential for future use in cancer therapy. Whether flavonoids bind directly to TMEM16A channels or through some other cellular mechanisms and act to modulate TMEM16A channels is presently unknown. TMEM16A channels should be included in the growing list of potential targets of flavonoids.

TMEM16A channels are not likely to be the sole mechanism responsible for flavonoid-associated anticancer effects, as flavonoids are reported to modulate many different ion channels (e.g. hERG K⁺ channels [Zitron *et al.,* 2005] and *ether á go-go 1* channels [Carlson *et al.,* 2013a,b]), which may be involved in progression of cancer. In addition, $Ca_v1.2$ channels (Saponara *et al.,* 2011), TRPC5 channels (Naylor *et al.,* 2016) and HCN2 channels (Carlson *et al.,* 2013a,b) are also modulated by flavonoids. Therefore, based on the results from this study, we consider that TMEM16A channels may play an important role in the anticancer effects associated with flavonoids.

Flavonoids have been reported to have a broad spectrum of biological activities including anticancer activity, through a variety of mechanisms. Based on our observation and others, in which flavonoids such as **luteolin**, **galangin**, **quercetin** and **fisetin** are able to interfere with almost all the aspects of carcinogenesis, it appears they are relatively safe to be used in humans or animals. Flavonoids are assumed to be potential chemopreventive agents against certain types of cancer *via* blockade of TMEM16A currents, in addition to

suppression of tumour proliferation and migration. Nevertheless, further prospective studies are needed to confirm the anticancer activities and the safety of flavonoids for use in cancer prevention and therapy in humans.

Author contributions

X.Z., H.L., H.Z., Y.L, L.H. and Y.X. performed the research. X.Z., Z.J. and W.Z. designed the research study. X.Z. and X.S. analysed the data. X.Z. and W.Z. wrote the paper.

Conflict of interest

The authors declare no conflicts of interest.

Declaration of transparency and scientific rigour

This Declaration acknowledges that this paper adheres to the principles for transparent reporting and scientific rigour of preclinical research recommended by funding agencies, publishers and other organisations engaged with supporting research.

References

Akervall JA, Jin Y, Wennerberg JP, Zatterstrom UK, Kjellen E, Mertens F *et al.* (1995). Chromosomal abnormalities involving 11q13 are associated with poor prognosis in patients with squamous cell carcinoma of the head and neck. Cancer 76: 853–859.

Alexander SPH, Kelly E, Marrion N, Peters JA, Benson HE, Faccenda E *et al.* (2015). The Concise Guide to PHARMACOLOGY 2015/16: Other ion channels. Br J Pharmacol 172: 5942–5955.

Arai Y, Watanabe S, Kimira M, Shimoi K, Mochizuki R, Kinae N (2000). Dietary intakes of flavonols, flavones and isoflavones by Japanese women and the inverse correlation between quercetin intake and plasma LDL cholesterol concentration. J Nutr 130: 2243–2250.

Britschgi A, Bill A, Brinkhaus H, Rothwell C, Clay I, Duss S *et al.* (2013). Calcium-activated chloride channel ANO1 promotes breast cancer progression by activating EGFR and CAMK signaling. Proc Natl Acad Sci U S A 110: E1026–E1034.

Caputo A, Caci E, Ferrera L, Pedemonte N, Barsanti C, Sondo E *et al.* (2008). TMEM16A, a membrane protein associated with calcium-dependent chloride channel activity. Science 322: 590–594.

Carlson AE, Brelidze TI, Zagotta WN (2013a). Flavonoid regulation of EAG1 channels. J Gen Physiol 141: 347–358.

Carlson AE, Rosenbaum JC, Brelidze TI, Klevit RE, Zagotta WN (2013b). Flavonoid regulation of HCN2 channels. J Biol Chem 288: 33136–33145.

Carneiro A, Isinger A, Karlsson A, Johansson J, Jonsson G, Bendahl PO *et al.* (2008). Prognostic impact of array-based genomic profiles in esophageal squamous cell cancer. BMC Cancer 8: 98.

Croft KD (1998). The chemistry and biological effects of flavonoids and phenolic acids. Ann N Y Acad Sci 854: 435–442.

Curtis MJ, Bond RA, Spina D, Ahluwalia A, Alexander SP, Giembycz MA *et al.* (2015). Experimental design and analysis and their reporting: new guidance for publication in BJP. Br J Pharmacol 172: 3461–3471.

De La Fuente R, Namkung W, Mills A, Verkman AS (2008). Small-molecule screen identifies inhibitors of a human intestinal calcium-activated chloride channel. Mol Pharmacol 73: 758–768.

Duvvuri U, Shiwarski DJ, Xiao D, Bertrand C, Huang X, Edinger RS *et al.* (2012). TMEM16A induces MAPK and contributes directly to tumorigenesis and cancer progression. Cancer Res 72: 3270–3281.

Garcia-Closas R, Agudo A, Gonzalez CA, Riboli E (1998). Intake of specific carotenoids and flavonoids and the risk of lung cancer in women in Barcelona, Spain. Nutr Cancer 32: 154–158.

Gim H, Nam JH, Lee S, Shim JH, Kim HJ, Ha KT *et al.* (2015). Quercetin inhibits pacemaker potentials via nitric oxide/cGMP-dependent activation and TRPM7/ANO1 channels in cultured interstitial cells of cajal from mouse small intestine. Cell Physiol Biochem 35: 2422–2436.

Helix N, Strobaek D, Dahl BH, Christophersen P (2003). Inhibition of the endogenous volume-regulated anion channel (VRAC) in HEK293 cells by acidic di-aryl-ureas. J Membr Biol 196: 83–94.

Hirvonen T, Virtamo J, Korhonen P, Albanes D, Pietinen P (2001). Flavonol and flavone intake and the risk of cancer in male smokers (Finland). Cancer Causes Control 12: 789–796.

Knekt P, Jarvinen R, Seppanen R, Hellovaara M, Teppo L, Pukkala E *et al.* (1997). Dietary flavonoids and the risk of lung cancer and other malignant neoplasms. Am J Epidemiol 146: 223–230.

Li H, Yan X, Li R, Zhang A, Niu Z, Cai Z *et al.* (2016). Increased TMEM16A involved in alveolar fluid clearance after lipopolysaccharide stimulation. Inflammation 39: 881–890.

Liantonio A, Pusch M, Picollo A, Guida P, De Luca A, Pierno S *et al.* (2004). Investigations of pharmacologic properties of the renal CLC-K1 chloride channel co-expressed with barttin by the use of 2-(p-Chlorophenoxy)propionic acid derivatives and other structurally unrelated chloride channels blockers. J Am Soc Nephrol 15: 13–20.

Liu F, Cao QH, Lu DJ, Luo B, Lu XF, Luo RC *et al.* (2015). TMEM16A overexpression contributes to tumor invasion and poor prognosis of human gastric cancer through TGF-beta signaling. Oncotarget 6: 11585–11599.

Liu Y, Zhang H, Huang D, Qi J, Xu J, Gao H *et al.* (2014). Characterization of the effects of Cl(−) channel modulators on TMEM16A and bestrophin-1 Ca(2)(+) activated Cl(−) channels. Pflugers Arch 467: 1417–1430.

Mazzone A, Eisenman ST, Strege PR, Yao Z, Ordog T, Gibbons SJ *et al.* (2012). Inhibition of cell proliferation by a selective inhibitor of the Ca(2+)-activated Cl(−) channel, Ano1. Biochem Biophys Res Commun 427: 248–253.

Namkung W, Phuan PW, Verkman AS (2010a). TMEM16A inhibitors reveal TMEM16A as a minor component of calcium-activated chloride channel conductance in airway and intestinal epithelial cells. J Biol Chem 286: 2365–2374.

Namkung W, Thiagarajah JR, Phuan PW, Verkman AS (2010b). Inhibition of Ca^{2+}-activated Cl$^-$ channels by gallotannins as a possible molecular basis for health benefits of red wine and green tea. FASEB J 24: 4178–4186.

Naylor J, Minard A, Gaunt HJ, Amer MS, Wilson LA, Migliore M *et al.* (2016). Natural and synthetic flavonoid modulation of TRPC5 channels. Br J Pharmacol 173: 562–574.

Neuhouser ML (2004). Dietary flavonoids and cancer risk: evidence from human population studies. Nutr Cancer 50: 1–7.

Parkerson KA, Sontheimer H (2004). Biophysical and pharmacological characterization of hypotonically activated chloride currents in cortical astrocytes. Glia 46: 419–436.

Picollo A, Liantonio A, Didonna MP, Elia L, Camerino DC, Pusch M (2004). Molecular determinants of differential pore blocking of kidney CLC-K chloride channels. EMBO Rep 5: 584–589.

Qu Z, Yao W, Yao R, Liu X, Yu K, Hartzell C (2014). The Ca(2+)-activated Cl(−) channel, ANO1 (TMEM16A), is a double-edged sword in cell proliferation and tumorigenesis. Cancer Med 3: 453–461.

Ruppersburg CC, Hartzell HC (2014). The Ca^{2+}-activated Cl$^-$ channel ANO1/TMEM16A regulates primary ciliogenesis. Mol Biol Cell 25: 1793–1807.

Saponara S, Carosati E, Mugnai P, Sgaragli G, Fusi F (2011). The flavonoid scaffold as a template for the design of modulators of the vascular Cav1.2 channels. Br J Pharmacol 164: 1684–1697.

Schroeder BC, Cheng T, Jan YN, Jan LY (2008). Expression cloning of TMEM16A as a calcium-activated chloride channel subunit. Cell 134: 1019–1029.

Southan C, Sharman JL, Benson HE, Faccenda E, Pawson AJ, Alexander SPH *et al.* (2016). The IUPHAR/BPS Guide to PHARMACOLOGY in 2016: towards curated quantitative interactions between 1300 protein targets and 6000 ligands. Nucl Acids Res 44 (Database Issue): D1054–D1068.

West RB, Corless CL, Chen X, Rubin BP, Subramanian S, Montgomery K *et al.* (2004). The novel marker, DOG1, is expressed ubiquitously in gastrointestinal stromal tumors irrespective of KIT or PDGFRA mutation status. Am J Pathol 165: 107–113.

Wright ME, Mayne ST, Stolzenberg-Solomon RZ, Li Z, Pietinen P, Taylor PR *et al.* (2004). Development of a comprehensive dietary antioxidant index and application to lung cancer risk in a cohort of male smokers. Am J Epidemiol 160: 68–76.

Yang YD, Cho H, Koo JY, Tak MH, Cho Y, Shim WS *et al.* (2008). TMEM16A confers receptor-activated calcium-dependent chloride conductance. Nature 455: 1210–1215.

Zhang H, Cao HJ, Kimelberg HK, Zhou M (2011). Volume regulated anion channel currents of rat hippocampal neurons and their contribution to oxygen-and-glucose deprivation induced neuronal death. PLoS One 6: e16803.

Zhang X, Du XN, Zhang GH, Jia ZF, Chen XJ, Huang DY *et al.* (2012). Agonist-dependent potentiation of vanilloid receptor transient receptor potential vanilloid type 1 function by stilbene derivatives. Mol Pharmacol 81: 689–700.

Zitron E, Scholz E, Owen R, Luck S, Kiesecker C, Thomas D *et al.* (2005). QTc prolongation by grapefruit juice and its potential pharmacological basis: HERG channel blockade by flavonoids. Circulation 111: 835–838.

Supporting Information

Additional Supporting Information may be found online in the supporting information tab for this article.

https://doi.org/10.1111/bph.13841

Figure S1 The effects of T16A$_{inh}$-A01 and CaCC$_{inh}$-A01 on recombinant TMEM16A currents in CHO cells. (A) Chemical structures of T16A$_{inh}$-A01. (B) Chemical structures of CaCC$_{inh}$-A01. (C) The time course for the effects of T16A$_{inh}$-A01 and CaCC$_{inh}$-A01 (all at 100 μM) on TMEM16A currents tested at +100 mV. The protocol was shown at the top of the figure. (D) The representative current traces recorded when the effect of drugs has stabilized.

Figure S2 The effects of Gala on TMEM16A currents is reversible. (A) The time course for the effects of Gala (30 μM) on TMEM16A currents tested at +100 mV. (B) The representative current traces recorded under different conditions of the treatments were shown.

Figure S3 The effects of Quer on deactivation kinetics of TMEM16A currents in LA795 cells. (A) The effects of Quer on the deactivation kinetics of TMEM16A currents from +100 to −100 mV. The red line shows the deactivating currents in the presence of the drugs, which were scaled up to match the amplitude of the deactivating currents in the absence of the drugs. (B) Summary of effects of Quer on the time constants of TMEM16A deactivating currents. *$P < 0.05$ compared with control, $n = 5$.